Materials Research Proceedings 41 (2024) 1817-1826 https://doi.org/10.21741/9781644903131-201

Intelligent control of ISBM process for recycled PET bottles

HAN William[1,a *], KERFRIDEN Pierre[1,b *], VIORA Laurianne[2,c], COMBEAUD Christelle[2,d], BOUVARD Jean-Luc[2,e], and CANTOURNET Sabine[1,f]

[1]Mines Paris, PSL University, Centre des Matériaux (CMAT), CNRS UMR 7633, BP 87, 91003 Evry, France

[2]Mines Paris, PSL University, Centre for Material Forming (CEMEF), UMR CNRS 7635, 1 rue Claude Daunesse, CS 10207, 06904 Sophia Antipolis, France

[a]william.han@minesparis.psl.eu, [b]pierre.kerfriden@minesparis.psl.eu, [c]laurianne.viora@minesparis.psl.eu, [d]christelle.combeaud@minesparis.psl.eu, [e]jean-luc.bouvard@minesparis.psl.eu, [f]sabine.cantournet@minesparis.psl.eu

Keywords: PET, Free Injection Stretch Blow Process, Machine Learning, Gaussian Process Regression

Abstract. To manufacture plastic bottles with an increased ratio of rPET (recycled Polyethylene terephthalate), the ISBM (Injection Stretch Blow Moulding) process must be controlled to account for the variable mechanical and thermal properties. Calibration and optimization of the process have been successfully realized in past works but cannot be used for real-time applications. To address this, a gaussian process regression model of the free blowing step is created. It can calibrate itself using the pressure curve from a previous blowing to obtain near instantaneous predictions of key properties of the bottle. To create the model, the process' characteristics are studied. Finite element simulations of the blowing where the properties follow a multivariate gaussian distribution are used to train the artificial intelligence. Then, an example is shown using the artificial intelligence predictions to optimize the thickness distribution of a bottle after blowing.

Introduction

To manufacture plastic bottles, ISBM (Injection Stretch Blow Moulding) is the most employed process. PET (Polyethylene terephthalate) is commonly used for food packaging because of its advantageous mechanical, optical and barrier properties. To improve sustainability, usage of rPET for bottle forming is currently increasing.

Past studies have considered the simulation of the blowing step of the ISBM process [1,2] to help reducing costs in optimizing the process. However, the complex models used to produce accurate predictions make the simulations very expensive [3], and therefore, the time needed for calibration and optimization makes on-line control of the process unpractical.

It is especially true when considering rPET (recycled PET), since adding recycled PET will affect the mechanical and thermal properties of the preform [4,5] and disturb the high-paced production line (1.5 s per bottle from start to finish [6]). Therefore, to increase the ratio of recycled resin, it is necessary to be able to adapt the process to the varying amount of rPET.

In this study, we propose a method inspired by digital twinning methods devised recently [7,8] to drastically reduce the time needed for calibration and optimization. To do this, an AI (artificial intelligence) model is constructed to be able to predict outputs of the calibrated model given control inputs and historical process signature.

To illustrate this, we focus on the free blowing step to simplify the process. First, the settings of the process are enunciated following literature and real behaviour as much as possible. Then, a procedure to train an AI model to give quick prediction of a self-calibrated model is presented. Finally, the capability of the model is showcased by doing an optimization of the process.

1. Free blowing process

The study focuses on a simplified blowing step spanning 0.3 s and realized with no mould (free blowing).

Optimization of the bottle thickness distribution has been a focus of previous studies [9,10] because of its importance to have uniform properties throughout the bottle [6]. Since there is no mould in the study, the volume of the bottle formed is not controlled. Therefore, to optimize the thickness homogeneity, we aim to minimize the standard deviation of the bottle thickness distribution σ_{Wd} for a given volume V_f.

The process is usually controlled by the injection pressure and how much heating energy is applied to the preform. Salomeia et al. [11] have shown that the injection pressure results in a choked flow, thus constant mass air flow Q_{air} when the ratio between the internal pressure and the injection pressure is low enough. To simplify the problem, we consider the process controlled by a constant temperature T throughout the preform and the blowing duration. The range of both control parameters is consistent with usual values in the literature [2,12].

Table 1. Control parameters and their range.

Control Parameters (μ)	**Range**
Mass air flow Q_{air} [g s^{-1}]	$[10, 30]$
Temperature T [°C]	$[85, 120]$

The preform is an 18.5 g preform following a geometry used by SIDEL, partner of the CARNOT 2020 AAP 2 BOUTEILLE project (Figure 1). The material is PET with varying amount of recycled PET.

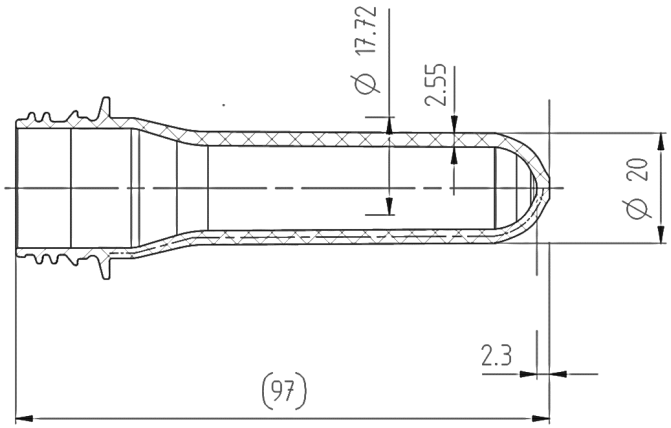

Fig. 1. Preform design.

To monitor the process, the preform internal pressure is recorded during the blowing step. Indeed, past studies suggest that the behaviour pressure history is closely related to the course and characteristics of the process [1,13].

2. Uncertainties in the free blowing problem

In the process, there are several parameters that are not known beforehand, but will have a noticeable impact on the process control. In Table 2, such parameters are compiled with their expected standard deviations. They include the lack of accuracy of the sensors or the controls of the process, the environmental conditions for the bottle internal pressure P, mass air flow Q_{air} and

temperature T measurements, and the thickness deviation from the specified thickness distribution $\boldsymbol{W_d}$.

To evaluate the variance caused by the presence of recycled PET, measurements for the storage modulus E' were realized by Viora et al. [5] by DMA using samples with three different ratios of recycled PET (0%, 50% or 100%). Temperature scans were realized between 25°C and 140°C, with a heating rate of 2 °C/min, at a frequency of 1 Hz, a preload of 1 N and a dynamic deformation of 0.04%. Five scans of the storage modulus are shown in Figure 2 and show the variations between different types, with a tendency for PET with lesser amounts of recycled resin to be more rigid in the rubbery plateau (around 90°C-115°C). It also shows that material variations seem to have a logarithmic distribution. Therefore, for the material variations, a geometric standard deviation factor $\sigma_m(T)$ was calculated (eq. 1) using $\overline{E'(T)}$ the geometric mean of the measurements $E'_i(T)$ at temperature T.

$$\sigma_m(T) = \exp\sqrt{\frac{1}{n}\sum_{i=1}^{n}\left(\ln\frac{E'_i(T)}{\overline{E'(T)}}\right)} \quad (1)$$

To simplify, the arithmetic average $\overline{\sigma_m}$ of $\sigma_m(T)$ at temperatures between 85°C and 120°C was chosen.

Table 2. Error between the expected value and reality.

Uncertain parameters	Standard deviation
Bottle internal pressure	$\sigma_P = 0.25\%$
Mass air flow	$\sigma_{Q_{air}} = 2.5\%$
Temperature	$\sigma_T = 1°C$
Geometry (thickness)	$\sigma_w = 0.01$ mm
Material	$\overline{\sigma_m} = 0.116$

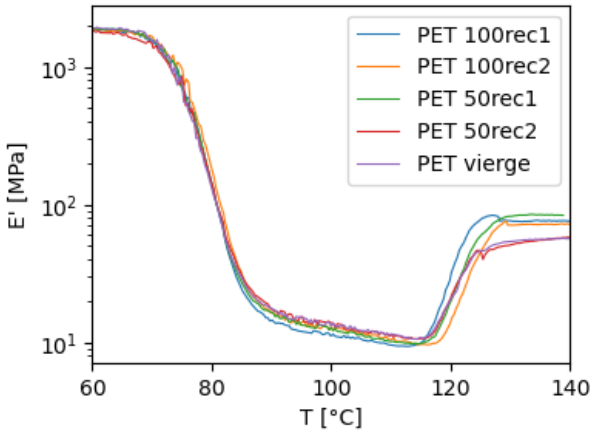

Fig. 2. Storage modulus (E') as a function of temperature for different samples, in tensile mode, at a frequency of 1 Hz and a heating rate of 2°C/min.

3. Methodology

The gaussian process regression machine learning model is presented here, alongside the data used to train it.

Gaussian Process Regression (GPR). The blowing process has uncertainties which have been initially quantified. Assuming they follow a multivariate gaussian distribution, their knowledge can be carried in predictions by employing gaussian process regression machine learning [14]. Indeed, considering a point $\boldsymbol{x}$ in the input matrix $\mathbf{X}$, a prediction $f(\boldsymbol{x}) = \tilde{f}(\boldsymbol{x}) + \epsilon$ with a noise ϵ that quantify its uncertainty and $\tilde{f}(\boldsymbol{x})$ a gaussian process. To set up the prior distribution, $\tilde{f}(\boldsymbol{x})$ follows a covariance function K (eq.2) which was chosen to be the product of its amplitude A with a radial basis function kernel. It depends on the characteristic length-scale l and the distance between the input points $\boldsymbol{x_i}$ and $\boldsymbol{x_j}$.

$$K(\boldsymbol{x_i}, \boldsymbol{x_j}) = A \exp\left(-\frac{d(\boldsymbol{x_i}, \boldsymbol{x_j})^2}{2l_{ij}^2}\right) \tag{2}$$

The covariance function follows eq.3, where δ_{ij} is a Kronecker delta which is one if $i = j$ and zero otherwise and σ_n^2 the variance of the noise.

$$\operatorname{cov}\left(f(\boldsymbol{x_i}), f(\boldsymbol{x_j})\right) = K(\boldsymbol{x_i}, \boldsymbol{x_j}) + \sigma_n^2 \delta_{ij} \tag{3}$$

With $\boldsymbol{y} = f(\boldsymbol{x})$ the output vector, predictions from test points $\mathbf{X}^*$ will consequently have the following gaussian distribution:

$$\begin{aligned} &\boldsymbol{f}_*|\{f(x_i) = y_i\}_{i\leq n} \sim \mathcal{N}\left(\bar{\boldsymbol{f}}_*,\ cov(\boldsymbol{f}_*)\right) \\ &\bar{\boldsymbol{f}}_* = \mathbf{K}(\mathbf{X}_*, \mathbf{X})[\mathbf{K}(\mathbf{X}, \mathbf{X}) + \sigma_n^2 \mathbf{I}]^{-1} \boldsymbol{y} \\ &cov(\boldsymbol{f}_*) = \mathbf{K}(\mathbf{X}_*, \mathbf{X}_*) - \mathbf{K}(\mathbf{X}_*, \mathbf{X})[\mathbf{K}(\mathbf{X}, \mathbf{X}) + \sigma_n^2 \mathbf{I}]^{-1} \mathbf{K}(\mathbf{X}, \mathbf{X}_*) \end{aligned} \tag{4}$$

The parameters $\boldsymbol{l}$, A, and σ_n are determined from data by maximizing the log-likelihood:

$$\ln P(y) = -\frac{1}{2}\ln\det(\mathbf{K}(\mathbf{X}, \mathbf{X}) + \sigma_n^2 \mathbf{I}) - \frac{1}{2} y^T (\mathbf{K}(\mathbf{X}, \mathbf{X}) + \sigma_n^2 \mathbf{I})^{-1} y - \frac{N}{2}\ln(2\pi) \tag{5}$$

Simulations. The training data was constructed using free blowing simulations using Abaqus/Explicit. Similarly to previous studies [1,2,9], they are conducted with the fluid cavity option, where a basic fluid-structure interaction is calculated between the air modelled as an ideal gas and the preform. Simulations were performed with 84 axisymmetric shell elements (SAX1) following the inner surface of the preform. Rigid elements (RAX2) were used at the base of the preform to close the cavity.

The Arruda-Boyce incompressible hyperelastic material law was chosen for its simplicity, fast computation ($\sim$30 s per simulation) and its ability to reproduce the bottle shape during the blowing step (Figure 3).

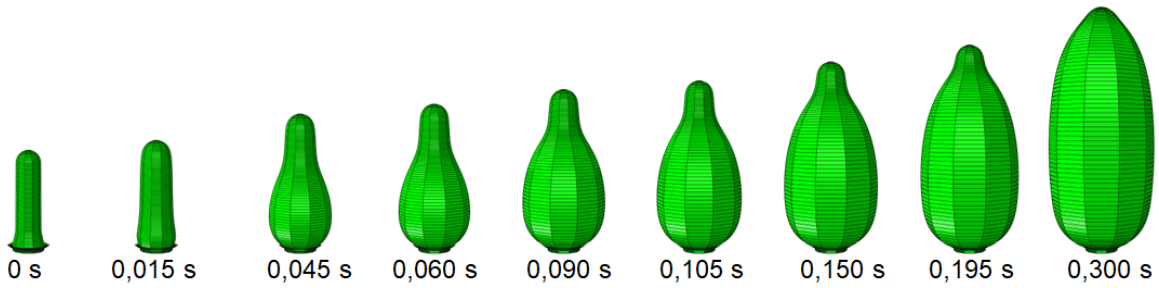

Fig. 3. Free blow simulation with an air mass flow of $\mathbf{14\ g\ s^{-1}}$, *(*$\boldsymbol{\mu_r = 5.6\ MPa}$, $\boldsymbol{\lambda_m = 3}$*).*

Its strain energy density is given by eq. 6 where $\lambda_{chain} = \sqrt{I_1/3}$ with I_1 the first invariant of the left Cauchy-Green deformation tensor, and $\beta = \mathcal{L}^{-1}(\lambda_{chain}/\lambda_m)$ with $\mathcal{L}(\beta) = \coth(\beta) - 1/\beta$ the Langevin function. It depends on two parameters, the shear modulus μ_r and λ_m which is the stretch at which the polymer chain network becomes locked.

$$W = G\left(\lambda_m \lambda_{chain}\beta + \lambda_m^2 \ln\frac{\sinh\beta}{\beta}\right) \tag{6}$$

A rudimentary temperature dependency is inputted in the simulation through the material law. Since we consider the PET incompressible, $G = E'/\big(2(1+\nu)\big) = E'/3$. Thus, to obtain the average shear modulus $\overline{G(T)}$, an empirical model for $\overline{E'(T)}$ (eq.7) was fitted using the average curve of the DMA data described in section 2.

$$\overline{E'(T)} = A_0 \exp\left(-KT + B_1 \tanh\left(\frac{T_1 - T}{T_1^*}\right) + B_2 \tanh\left(\frac{T - T_2}{T_2^*}\right)\right) \tag{7}$$

Since no data was readily available to identify λ_m, the limit of the viscous strain values measured by Chevalier et al. [15] were used to fit a model (eq. 8). A sigmoid was used to avoid values getting too high as the blowing behaviour already tends to neo-Hookean when $\lambda_m > 5$.

$$\overline{\lambda_m(T)} = (A_\lambda T + B_\lambda)\left(1 + \frac{2}{1+\exp(T - T_\lambda)}\right) \tag{8}$$

Table 3. Identified parameters of eq.7 and 8.

Parameters of eq.7	A_0	K	B_1	T_1	T_1^*	B_2	T_2	T_2^*
	1476 MPa	0.01704 °C^{-1}	2.242	79.64 °C	5.461 °C	0.7846	119.7 °C	2.87°C
Parameters of eq. 8	A_λ	B_λ	T_λ					
	0.0184	0.306	111°C					

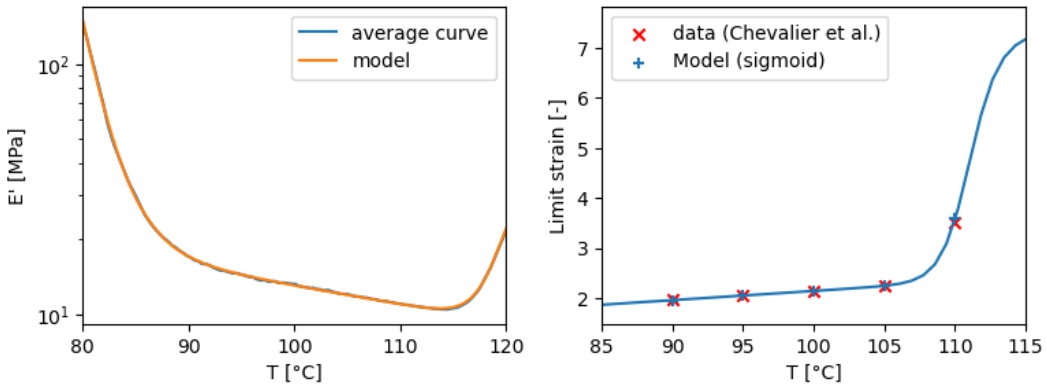

Fig. 4. Comparison of experimental data and eq. 7 (left) and eq. 8 (right).

Construction of the training data. To create an input point $\boldsymbol{x}$ in the training data, a simulation is done to record the internal pressure history. However, since the pressure history $\boldsymbol{P}$ will change depending on the controls $\boldsymbol{\mu}$ used to obtain it, it cannot serve alone as the process signature in a problem where the optimization is realized on those same controls. Hence, the internal pressure history $\boldsymbol{P_1}$ is recorded alongside the control $\boldsymbol{\mu_1} = (Q_{air_1}, T_1)$ to have the process signature $(\boldsymbol{P_1}, \boldsymbol{\mu_1})$ and let the model learn the relationship $\boldsymbol{P_1}(\boldsymbol{\mu_1})$ to calibrate the predictions. Then, a second simulation is needed to link the control $\boldsymbol{\mu_2} = (Q_{air_2}, T_2)$ to the quantities $\boldsymbol{y} = (V_f, \sigma_w)$ we wish to predict. Two simulations were needed as the pressure curve $\boldsymbol{P}$ depends on the control parameters $\boldsymbol{\mu}$ and therefore is not enough alone to constitute the process signature allowing for model calibration. To keep a reasonable dimensionality for the problem, we reduced the pressure history to a vector with three characteristic values ($\boldsymbol{\mathcal{P}_1} = (p_1^{\mathrm{I}}, p_1^{\mathrm{II}}, p_1^{\mathrm{III}})$) using principal component analysis. Therefore, the input vector $\boldsymbol{x} = (\boldsymbol{\mu_2}, \boldsymbol{\mathcal{P}_1}, \boldsymbol{\mu_1})$ is used to predict the output $\boldsymbol{y}$.

As such, in the range of Table 1, the $\boldsymbol{\mu_1}$ and $\boldsymbol{\mu_2}$ matrices were sampled using a Sobol sequence [16] to create a low-discrepancy distribution in the parameter space. Then, to include the knowledge of the process described in section 2, a matrix $\boldsymbol{\Theta}$ was constructed so that a distribution $\boldsymbol{\theta_k} \in \boldsymbol{\Theta}$ (with $k \in \{P, Q_{air}, T, w, G, \lambda_m\}$) represents the true values that are unknown either because of measurement inaccuracy, or because they are not measured. The distributions for each unknown parameter are described in Table 4, where $\boldsymbol{Z_k} \sim \mathcal{N}(0,1)$ are random distributions following the unitary normal law. As the two simulations used for an input point are part of the same process, we considered that $\boldsymbol{Z_k} = \boldsymbol{Z_{1,k}} = \boldsymbol{Z_{2,k}}$.

Table 4. Error between the expected value and reality.

Unknown parameters	**Distribution**
True bottle internal pressure	$\boldsymbol{\theta_P} = \boldsymbol{P}(1 + \sigma_P \boldsymbol{Z_P})$
True mass air flow	$\boldsymbol{\theta_{Q_{air}}} = \boldsymbol{Q_{air}}(1 + \sigma_{Q_{air}} \boldsymbol{Z_{Q_{air}}})$
True temperature	$\boldsymbol{\theta_T} = \boldsymbol{T} + \sigma_T \boldsymbol{Z_T}$
Geometry (thickness)	$\boldsymbol{\theta_w} = \boldsymbol{W_d} + \sigma_w \boldsymbol{Z_w}$
Material (G)	$\boldsymbol{\theta_G} = \frac{1}{3}\exp\left(\log\left(\overline{E'(\boldsymbol{T})}\right) + \sigma_m \boldsymbol{Z_{E'}}\right)$
Material (λ_m)	$\boldsymbol{\theta_{\lambda_m}} = \exp\left(\log\left(\overline{\lambda_m(\boldsymbol{T})}\right) + \sigma_m \boldsymbol{Z_{\lambda_m}}\right)$

Thus, to create the training data, the simulations were controlled by the matrices $\boldsymbol{\Theta_1}$ and $\boldsymbol{\Theta_2}$ for all parameters aside from the bottle internal pressure (since $\boldsymbol{\theta_P}$ is the simulation result, $\boldsymbol{P}$ is calculated afterward).

Training results. The training input and output $\mathbf{X_{train}}$ and $\mathbf{Y_{train}}$ was constructed with 10000 points from 20000 simulations. Two gaussian processes to respectively predict V_f and σ_{W_d} were trained with the scikit-learn [17] implementation of gaussian process regression. To evaluate the generalization capability of the model, test data ($\mathbf{X_{test}}$, $\mathbf{Y_{test}}$) was also constructed with 1000 different points obtained in a similar manner as for the training data. The performance was rated by how many points are inside the 95% confidence interval of the prediction's distribution. Table 5 shows that the training goes well since around 95% of the predictions are indeed in the 95% confidence interval and that the model generalizes satisfactorily since the percentage of unknown data in the prediction's confidence interval is only slightly lower.

*Table 5. Ratio of output data **Y** inside the 95% confidence interval.*

Quantity of interest	Training results	Test results
Volume V_f	95.33%	93.7%
Thickness SD σ_w	94.69%	93.7%

4. Test of the model: robust optimization of the control parameters

In Figure 5, the result of a blowing taken from the validation set is shown, alongside its thickness distribution. The control parameters used were $Q_{air} = 14.8\ \mathrm{g\ s^{-1}}$ and $T = 111°\mathrm{C}$. The bubble only formed at the base of the preform, thus the membrane is still very thick (~2.5 mm) at the top. As the base of the preform is clamped, the material stays thick in that area. The final volume obtained was $V_f = 1.74$ L with a thickness standard deviation $\sigma_{Wd} = 1.05$ mm. To demonstrate the capability of the model, in this section, the aim is to optimize the controls to have a two-litre bottle with a more uniform thickness distribution.

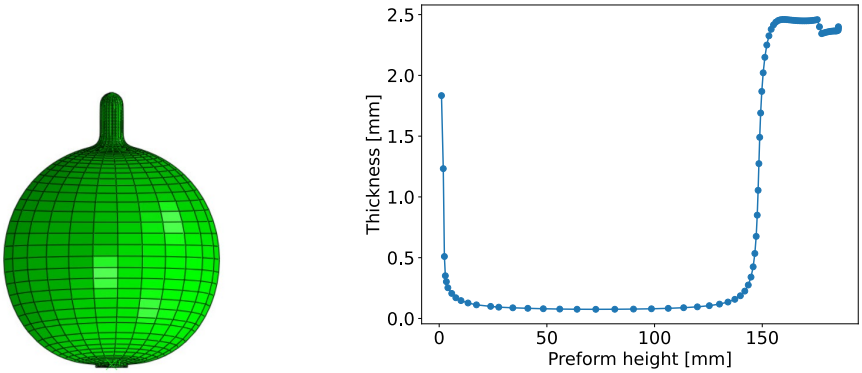

Fig. 5. Final shape of the bottle blown with $\boldsymbol{Q_{air} = 14.8\ g\ s^{-1}, T = 111°C}$ (left), thickness distribution of the bottle (right).

Objective function. To obtain a more uniform thickness distribution, the objective function aims to minimize the standard deviation of the thickness. As $\boldsymbol{\mathcal{P}_1}$ and $\boldsymbol{\mu_1}$ are here to calibrate the model, the minimization is realized on $\boldsymbol{\mu_2}$. Since there is no mould, a constraint was added to define the desired volume of the bottle. The gaussian process regression method gives predictions in the form of distribution, thus the uncertainty on the volume prediction can also be accounted for. In eq.9, $V_{f,obj}$ is the desired volume, ε_V is the volume error tolerance, $\mathbb{P}_v$ is the probability of having $V_f \in \left[V_{f,obj} - \varepsilon_V, V_{f,obj} + \varepsilon_V\right]$, and $\mathbb{P}_m$ is the minimal probability tolerated on the predicted volume being in the accepted error margin.

$$\min_{\boldsymbol{\mu_2}} \sigma_{Wd}\left(\boldsymbol{x}(\boldsymbol{\mu_2}, \boldsymbol{\mathcal{P}_1}, \boldsymbol{\mu_1})\right)$$
$$\mathbb{P}_v(\boldsymbol{\mu_2}) = \mathbb{P}\left(\left|V_{f,obj} - V_f\left(\boldsymbol{x}(\boldsymbol{\mu_2}, \boldsymbol{\mathcal{P}_1}, \boldsymbol{\mu_1})\right)\right| < \varepsilon_V\right) > \mathbb{P}_m \quad (9)$$

Optimization results. The optimization was realized using the trained machine learning model to evaluate σ_w and V_f, with the differential evolution method [18] integrated in SciPy. In eq. 9, the following parameters were set: $\varepsilon_V = 0.2$, $\mathbb{P}_m = 70\%$ and $V_f = 2$ L. $\mathbb{P}_m$ is taken low because preliminary calculations of probabilities to obtain the desired volume did not go above 73.5%. Optimized control parameters given by the algorithm were $Q_{air} = 29.5\ \mathrm{g\ s^{-1}}$ and $T = 107.7$°C. A volume of $V_f = 1.84$ L is obtained, which is inside the range of the volume constraint. The thickness standard deviation is $\sigma_{Wd} = 0.59$ mm which is much lower than the original standard deviation. The results with optimized controls are presented in Figure 6. This time, the bubble at the base of the preform has propagated to nearly the whole preform, thus a thickness higher than 2 mm can only be observed at the end of the preform.

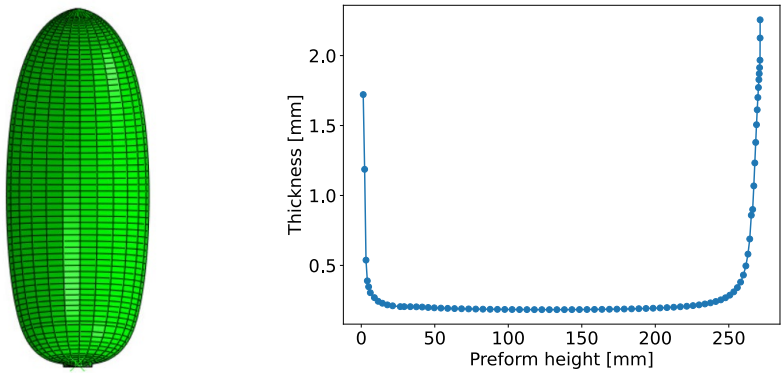

Fig. 6. Final shape of the bottle blown with optimized parameters $\boldsymbol{Q_{air} = 29.5\ g\ m^{-3}, T = 107.7°C}$ *(left), thickness distribution of the bottle (right).*

The optimization took 213 s and evaluated the objective function 1717 times. This is way faster than optimization using finite element simulation, as calibration of the process is already done, and even with simulations lasting one minute, the optimization would have taken 30 hours.

Conclusion

In this study, a methodology able to adapt its results depending on PETs with different ratio of rPET and depending on the conditions of the process was presented. Gaussian process regression models were trained using free blowing simulations following the Arruda-Boyce model, where the variability of the parameters was determined according to the variability of DMTA measurements obtained using resin with different ratios of rPET. It was able to provide a very fast optimization of the blowing process of a bottle.

For future works, the aim will be to improve the physical model of the simulations used for training. The viscoplasticity of the PET and the influence of the heating conditions of the bottle will notably have to be implemented to obtain more realistic predictions. To improve the precision of the predictions, the influence of the size of the training database, and the influence of the bottle blowing history of the process should be studied.

Nomenclature

x Scalar
$\boldsymbol{x}$ Vector
$\mathbf{x}$ Matrix

Acknowledgments
The authors gratefully acknowledge the financial support from ARMINES organization for the CARNOT MINES 2020 on Polymer recyclability.

References

[1] J. Nixon, G.H. Menary, S. Yan, Finite element simulations of stretch-blow moulding with experimental validation over a broad process window, Int. J. Mater. Form. 10 (2017) 793–809. https://doi.org/10.1007/s12289-016-1320-9

[2] Y. Luo, L. Chevalier, E. Monteiro, S. Yan, G. Menary, Simulation of the Injection Stretch Blow Molding Process: An Anisotropic Visco-Hyperelastic Model for Polyethylene Terephthalate Behavior, Polym. Eng. Sci. 60 (2020) 823–831. https://doi.org/10.1002/pen.25341

[3] Y. Luo, G. Tantchou Yakam, R. Charlot, L. Chevalier, R. Savajano, In situ adjustment of a visco hyper elastic model for stretch blow molding process simulation of poly-ethylene terephthalate bottles, Polym. Eng. Sci. 63 (2023) 3066–3082. https://doi.org/10.1002/pen.26428

[4] A.-D. Le, R. Gilblas, V. Lucin, Y.L. Maoult, F. Schmidt, Infrared heating modeling of recycled PET preforms in injection stretch blow molding process, Int. J. Therm. Sci. 181 (2022) 107762. https://doi.org/10.1016/j.ijthermalsci.2022.107762

[5] L. Viora, M. Combeau, M.F. Pucci, D. Perrin, P.-J. Liotier, J.-L. Bouvard, C. Combeaud, A Comparative Study on Crystallisation for Virgin and Recycled Polyethylene Terephthalate (PET): Multiscale Effects on Physico-Mechanical Properties, Polymers 15 (2023) 4613. https://doi.org/10.3390/polym15234613

[6] O. Brandau, Stretch blow molding, Third edition, William Andrew, an imprint of Elsevier, Amsterdam Boston Heidelberg, 2017.

[7] P.-B. Rubio, L. Chamoin, F. Louf, Real-time data assimilation and control on mechanical systems under uncertainties, Adv. Model. Simul. Eng. Sci. 8 (2021) 4. https://doi.org/10.1186/s40323-021-00188-3

[8] P. Pereira Álvarez, P. Kerfriden, D. Ryckelynck, V. Robin, Real-Time Data Assimilation in Welding Operations Using Thermal Imaging and Accelerated High-Fidelity Digital Twinning, Mathematics 9 (2021) 2263. https://doi.org/10.3390/math9182263

[9] M. Bordival, F.M. Schmidt, Y.L. Maoult, V. Velay, Optimization of preform temperature distribution for the stretch-blow molding of PET bottles: Infrared heating and blowing modeling, Polym. Eng. Sci. 49 (2009) 783–793. https://doi.org/10.1002/pen.21296

[10] J. Biglione, Y. Béreaux, J.-Y. Charmeau, J. Balcaen, S. Chhay, Numerical simulation and optimization of the injection blow molding of polypropylene bottles - a single stage process, Int. J. Mater. Form. 9 (2016) 471–487. https://doi.org/10.1007/s12289-015-1234-y

[11] Y. Salomeia, G.H. Menary, C.G. Armstrong, J. Nixon, S. Yan, Measuring and modelling air mass flow rate in the injection stretch blow moulding process, Int. J. Mater. Form. 9 (2015) 531–545. https://doi.org/10.1007/s12289-015-1240-0

[12] E. Gorlier, J.F. Agassant, J.M. Haudin, N. Billon, Experimental and theoretical study of uniaxial deformation of amorphous poly(ethylene terephthalate) above glass transition temperature, Plast. Rubber Compos. 30 (2001) 48–55. https://doi.org/10.1179/146580101101541435

[13] G.H. Menary, C.W. Tan, C.G. Armstrong, Y. Salomeia, M. Picard, N. Billon, E.M.A. Harkin-Jones, Validating injection stretch-blow molding simulation through free blow trials, Polym. Eng. Sci. 50 (2010) 1047–1057. https://doi.org/10.1002/pen.21555

[14] C.E. Rasmussen, C.K.I. Williams, Gaussian processes for machine learning, MIT Press, Cambridge, Mass, 2006.

[15] L. Chevalier, Y.M. Luo, E. Monteiro, G.H. Menary, On visco-elastic modelling of polyethylene terephthalate behaviour during multiaxial elongations slightly over the glass transition temperature, Mech. Mater. 52 (2012) 103–116. https://doi.org/10.1016/j.mechmat.2012.05.003

[16] I.M. Sobol', On the distribution of points in a cube and the approximate evaluation of integrals, USSR Comput. Math. Math. Phys. 7 (1967) 86–112. https://doi.org/10.1016/0041-5553(67)90144-9

[17] F. Pedregosa, G. Varoquaux, A. Gramfort, V. Michel, B. Thirion, O. Grisel, M. Blondel, P. Prettenhofer, R. Weiss, V. Dubourg, J. Vanderplas, A. Passos, D. Cournapeau, Scikit-learn: Machine Learning in Python, J. Mach. Learn. Res. 12 (n.d.) 2825--2830.

[18] R. Storn, K. Price, Differential Evolution - A simple and efficient adaptive scheme for global optimization over continuous spaces, J. Glob. Optim. 11 (1997) 341–359. https://doi.org/10.1023/A:1008202821328